Published OnlineFirst March 25, 2011; DOI: 10.1158/1535-7163.MCT-10-0902

Therapeutic Discovery

Molecular Cancer Therapeutics

High-Throughput Screen Identifies Novel Inhibitors of Cancer Biomarker α-Methylacyl Coenzyme A Racemase (AMACR/P504S)

Brice A.P. Wilson[1,3], Haofan Wang[2], Benjamin A. Nacev[1], Ronnie C. Mease[2], Jun O. Liu[1], Martin G. Pomper[1,2], and William B. Isaacs[1,3]

Abstract

α-methylacyl coenzyme A racemase (AMACR) is a metabolic enzyme whose overexpression has been shown to be a diagnostic indicator of prostatic adenocarcinoma and other solid tumors. Here, we confirm that attenuation of AMACR expression diminishes the growth of prostate cancer cell lines by using stably expressed short-hairpin RNA constructs. This observation strongly suggests that the AMACR enzyme may be a target for therapeutic inhibition in prostate cancer. To this end, we report here a novel assay capable of screening libraries of diverse small molecules for inhibitors of AMACR activity. This assay facilitated the screening of approximately 5,000 unique compounds and the discovery of 7 distinct chemical entities capable of inhibiting AMACR at low micromolar concentrations. The most potent inhibitor discovered is the seleno-organic compound ebselen oxide [inhibitory concentration (IC_{50}): 0.80 μmol/L]. The parent compound, ebselen (IC_{50}: 2.79 μmol/L), is a covalent inactivator of AMACR ($K_{I(inact)}$: 24 μmol/L). Two of the AMACR inhibitors are selectively toxic to prostate cancer cell lines (LAPC4/LNCaP/PC3) that express AMACR compared to a normal prostate fibroblast cell line (WPMY1) that does not express the protein. This report shows the first high-throughput screen for the discovery of novel AMACR inhibitors, characterizes the first nonsubstrate-based inhibitors, and validates that AMACR is a viable chemotherapeutic target *in vitro*. *Mol Cancer Ther; 10(5); 825–38. ©2011 AACR.*

Introduction

α-methylacyl coenzyme A racemase (AMACR, EC 5.1.99.4) is a cofactor-independent metabolic enzyme important for the catabolism of branch-chained fatty acids and the maturation of bile acids from cholesterol precursors (1). The natural substrates for AMACR include (2*R*)/(2*S*) pristanoyl coenzyme A (Pri-CoA; Fig. 1A) and the bile acid precursor molecule (25*R*)/(25*S*)-trihydroxycholestanoyl CoA (Fig. 1B; refs. 1–5). Acting upon its substrate, the enzyme catalyzes the bidirectional stereoconversion (from S to R and the reverse) of the α-methyl proton via a 1,1-proton transfer thought to proceed through an enolate intermediate (3, 6).

In mammals, branch chain lipids are acquired either directly through the degradation of chlorophyll into phytanic acid (ruminants) or by the intake of ruminant byproducts (milk, beef, etc.; refs. 1, 2). These lipids (and cholesterol precursors of bile acids) naturally occur as a racemic mixture, and their complete oxidation requires that they be in the *S*-conformation (1, 2). AMACR carries out that conversion before further oxidation. In addition to natural substrates, AMACR can catalyze the stereoconversion of ibuprofenyl CoA (Fig 1C) from its inactive *R*-conformer to its biologically active *S*-enantiomer (3).

Two crystal structures of the homologous AMACR from *Mycobacterium tuberculosis* have been published (7, 8). Structurally, this enzyme (43% homologous to AMACR by protein sequence) belongs to the type III CoA transferase superfamily of enzymes. The crystal structure indicates that the enzyme forms a dimer of interlocking dimers with the active site at the interface of the large domain of 1 monomer and the small domain of the other monomer. The identified catalytic residues are H126 and D156 (homologous residues H122 and D152 in AMACR). The size and lack of prominent topography in the hydrophobic substrate binding pocket accommodates the binding of either enantiomer from a diverse array of substrates (Fig. 1; refs. 7, 8). A recent kinetic study of the recombinant human AMACR and a deuterium-labeled substrate observed that the rate of solvent

Authors' Affiliations: Departments of [1]Pharmacology and Molecular Sciences and [2]Radiology and Radiological Sciences, and [3]James Buchanan Brady Urological Institute, The Johns Hopkins University School of Medicine, Baltimore, Maryland.

Note: Supplementary material for this article is available at Molecular Cancer Therapeutics Online (http://mct.aacrjournals.org/).

Corresponding Authors: William B. Isaacs, Department of Urology, Johns Hopkins Hospital, Johns Hopkins University School of Medicine, 600 N. Wolfe Street, Marburg 115, Baltimore, MD 21287. Phone: 410-955-2518; Fax: 410-955-0833. E-mail: wisaacs@jhmi.edu

doi: 10.1158/1535-7163.MCT-10-0902

Published OnlineFirst March 25, 2011; DOI: 10.1158/1535-7163.MCT-10-0902

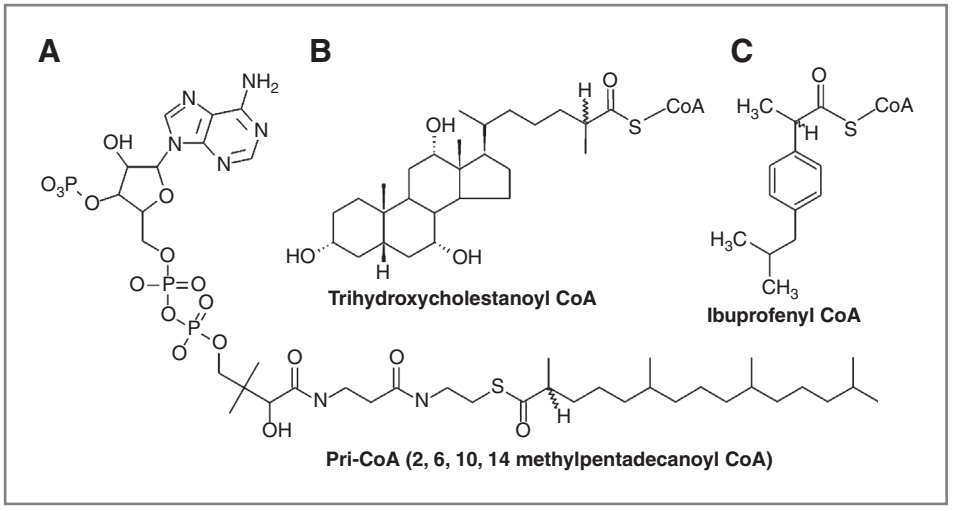

Figure 1. Well-characterized AMACR substrates. A, Pri-CoA [with complete chemical structure of CoA moiety]. B, THCA-CoA. C, ibuprofenyl CoA

exchange (without stereoconversion) is twice the rate of stereoconversion, implying that the mechanism of racemization is inefficient (3). This is consistent with data showing little to no preference for 1 chiral center (*R* or *S*) over the other.

Beyond its metabolic significance, AMACR is important in several human diseases. Patients with peroxisomal deficiency (Zellweger's syndrome) are deficient in AMACR activity (1), and patients with inactivating AMACR mutations (S52P and L107P) accumulate toxic levels of the *R*-conformer of branch chain fatty acids in their blood, resulting in neuropathy similar to Refsum disease (9). In addition, the specific upregulation of AMACR at both transcript and protein levels in prostatic adenocarcinoma and its precursor lesions, including putative prostate cancer progenitor populations, has been reported (10, 11, 12). Immunohistochemical detection of AMACR has become a valuable tool for the positive diagnosis of prostate cancer in tissue samples (11, 13). AMACR overexpression correlates with increased AMACR activity, indicating that the protein being expressed is enzymatically active and may be contributing to cancer growth (14, 15).

Decreasing the expression of AMACR through the use of short interfering RNA constructs has been shown to slow the growth of prostate cancer cell lines, indicating that not only may AMACR expression directly be supporting cancer growth but also that AMACR may be a new target for chemotherapeutic inhibition (14, 16). For targeted therapy, AMACR offers several advantages. First, an AMACR knockout mouse model has been generated and beyond the expected problem of branch chain lipid accumulation (safely regulated by diet alone), the mice have been reported to be healthy and fertile (17). This finding is in agreement with the observation that individuals with AMACR deficiency may remain asymptomatic for extended periods (9). Those data suggest that targeted inhibition of AMACR may offer promise as chemotherapy against prostate cancer without major inhibition-related side effects (14, 16). In addition to prostate cancer, AMACR has been shown to be overexpressed in a variety of solid tumors, suggesting that targeted inhibition may be translatable to other cancers (18).

In addition to exploiting the overexpression of AMACR for cancer chemotherapy, it is becoming increasingly clear that AMACR represents an excellent target for imaging of prostate cancer (19). While several imaging agents exist for detecting prostate cancer after it has disseminated, there is still a need for imaging agents to detect intraprostatic lesions (20, 21). Given that prostate cancer is the most commonly diagnosed cancer in men and the second leading cause of cancer-related death in men (22) and an increasing number of cases are being followed by active surveillance, finding imaging agents that target AMACR could represent an important advance for managing this disease (23, 24). An important distinction between AMACR and other candidate prostate cancer imaging targets is that AMACR expression is largely *cancer* specific, whereas *PSA* and *PSMA* are prostate specific, being expressed by both normal and cancerous prostate epithelial cells (20, 21).

There are few reported AMACR inhibitors. The scarcity of inhibitors relates in a large part to the unwieldy substrate requirements of the enzyme, namely: the presence of a CoA thioester (rendering the molecule impermeable to cells due to the presence of 3 phosphate molecules) and a minimum carbon chain length of 8 carbons (with the exception of ibuprofenyl CoA) for the acyl portion of the substrate (1, 2, 8). Multiple assays exist to quantify AMACR activity (1–8, 15, 25, 26). The most common assay relies on the production of radiolabeled water after incubation of AMACR with substrates containing tritium or deuterium at the α-position (1–3). Also, it is possible to monitor the stereoconversion of 1 enantiomer to another by incubating the enzyme with a stereochemically pure pool of substrate and then measuring the production of the opposite stereoisomer

Published OnlineFirst March 25, 2011; DOI: 10.1158/1535-7163.MCT-10-0902

after diastereomeric separation using either gas chromatography (GC) or high-performance liquid chromatography (HPLC; refs. 1–2, 6). By using these assays, inhibitors of AMACR activity have been identified [including mercury, copper (II), diethylpyrocarbonate (DEPC), Ellman's reagent, and *N*-ethylmaleimide; refs. 1, 2]. Recently, it has been shown that fluorine for hydrogen substitutions of known substrates near the α-position can result in the generation of competitive inhibitors. However, such molecules still require the presence of the CoA (SCoA) moiety, limiting their therapeutic potential (26).

While the aforementioned assays have single time point dependence, 2 continuous assays have been published (4, 25). One assay is an indirect coupled assay that monitors hydrogen peroxide production by the stereospecific oxidase immediately downstream of AMACR (25). That assay is limited in that it requires 2 different enzymes to be present, and a stereochemically pure substrate (25). Recently, a circular dichroism (CD) assay has been published (4). In this assay, the recombinant enzyme is incubated with stereochemically pure *R*- or *S*-ibuprofenyl CoA and CD measurements are made as the enzyme converts 1 diastereomer to the other (4). As with all prior assays for measuring AMACR activity or inhibition, the CD assay cannot be used to screen more than 1 reaction condition at a time. The arduous substrate (single optical isomers) or product preparations (diastereomer derivitization for analytic GC/HPLC separation) precludes the use of all existing assays in screening large libraries of diverse compounds.

We have designed a 96-well–based assay for the detection and testing of AMACR inhibitors. By using this assay, we discovered and subsequently characterized AMACR inhibitors that are not substrate-based. None of the inhibitors identified require the presence of the CoA moiety for activity, rendering them superior to previously identified compounds with respect to expected pharmacokinetic properties, thereby enabling further optimization and implementation *in vitro* and *in vivo*. Unlike previous inhibitors, these compounds do not behave in a competitive fashion, offering unique opportunities to gain insight into the structural requirements for AMACR inhibition. In addition, we report the development of the first stable AMACR knockdown cell line of prostate cancer cells (LAPC4-AMACRKO). These cells exhibit a statistically significant decreased growth rate and will offer an ideal syngeneic control for further AMACR-related *in vitro* and *in vivo* studies.

Materials and Methods

Reagents

Ebselen and ebselen oxide were purchased from Cayman Chemical Co., 3,7,12-trihydroxycholestanoic acid and pristanic acid from Larodan Fine Chemicals, CoA trilithium salt from MP Biomedicals, solid phase extraction (SPE) plates (Strata C18C) from Phenomenex, Inc., acetonitrile from ThermoFisher Scientific. [2, 3-^{3}H] Pri-CoA was synthesized by Moravek Biochemicals. Unless otherwise indicated, all other reagents were purchased from Sigma-Aldrich Corporation. All graphs and data analysis were accomplished by GraphPad Prism Software (GraphPad Software). All cell lines used have been authenticated as of November 2010 by short tandem repeat DNA analysis according to the manufacturer's protocol for the PowerPlex 1.2 System (Promega Corp.).

short-hairpin RNA–mediated AMACR knockdown

The human prostate cancer cell line LAPC4 was acquired from the laboratory of Dr. J.T. Isaacs (14). A total of 1×10^6 cells were plated in 100 mm dishes in normal culture media (Iscove's Modified Dulbecco's Media, Invitrogen Corp.) supplemented with 10% fetal bovine serum (Invitrogen) and 10 nm R1881 (PerkinElmer). The cells were allowed to establish and reach 80% confluency. The media were then replaced with fresh media containing 8 μg/mL hexadimethrine. Lentiviral transduction particles encoding short-hairpin RNA (shRNA) either targeting the AMACR transcript (AMACRKO, Sigma-Aldrich, clone ID TRCN0000084114) or not targeting any known human gene (vector control, Sigma-Aldrich, SHC002V) were added to this media. Cells were incubated with particles overnight before replacement with fresh media without hexadimethrine or particles. After a 24-hour recovery period, the media were exchanged for selection media containing 5 μg/mL puromycin and were allowed to undergo selection for 10 days before harvesting the entire population of viable cells and expanding them into a 300-mL tissue culture flask. Selection media were maintained henceforth.

After both the AMACRKO and the vector cell lines adequately expanded, Western blot analysis was done. Parental, AMACRKO, and vector cells were trypsinized, collected, washed with phosphate buffered saline (PBS) pH 7.4, and lyzed for 30 minutes in cell extraction buffer (Invitrogen). Insoluble material was spun down, and the lysate retained and quantified by the BCA Assay Kit (ThermoFisher). A total of 50 μg of each lysate was then loaded into adjacent wells in duplicate SDS-PAGE gels, 4%–20% gradient (ThermoFisher). The gels were electrophoresed according to manufacturer's protocols and were then transferred to nitrocellulose membranes for Western blotting. After electrophoretic transfer, 1.5 hours at 100 V, the blots were blocked for 30 minutes with blocking buffer (Li-Cor Biosciences). The membranes were then incubated with mouse anti-AMACR antibodies (1:2,000, Invitrogen) and rabbit antitubulin (1:10,000, Millipore Corp.) or mouse antiactin (1:25,000, Sigma-Aldrich) overnight at 4°C. The membranes were then washed with PBS (+0.1% Tween-20, USB Corp.) and incubated for 4 hours with antimouse and anti-rabbit or antimouse only secondary antibodies (1:25,000, Li-Cor). The membranes were then developed by the Li-Cor Odyssey infrared imaging system (Li-Cor). Cropped results are shown in the inset within Fig. 2 and

Published OnlineFirst March 25, 2011; DOI: 10.1158/1535-7163.MCT-10-0902

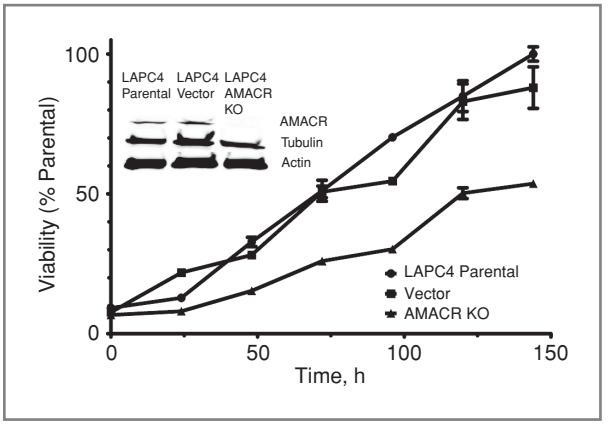

Figure 2. shRNA-mediated AMACR knockout in LAPC4 cells diminishes cell growth. Diminished AMACR expression affects cell growth as tested by the alamarBlue assay ($P < 0.005$, vector vs. AMACR KO, 2-tailed t test, $r = 0.9875$, $P = 0.2505$, vector vs. parental, $r = 0.9810$), all data points are normalized as a percentage of the maximum parental control. Inset, Western blot analysis showing AMACR expression in parental, vector control, and LAPC4 cells containing shRNA targeting AMACR protein. Tubulin and actin used as loading controls. AMACR is undetectable in AMACR KO cell line. Full-length blots in Supplementary Fig. S5.

the complete blots are included in the Supplementary Fig. S5.

To determine the effect that shRNA-mediated AMACR knockout has on cell growth and viability, LAPC4 parental, AMACRKO, and vector cells were assayed for their growth rate by the alamarBlue assay (AbD Serotec). A total of 5,000 cells of each type were plated in triplicate in 7 different tissue culture treated zero fluorescence 96-well plates (BD Biosciences) in 100 μL of media. Beginning with the initial plating and at subsequent 24 hour intervals, 10 μL alamarBlue reagent was added to each well (including media only controls) and incubated for 4 hours. The plate was then read on a Fluostar Omega plate reader (544 excitation/590 emission, BMG Labtech, Inc.), background fluorescence removed, and the change in fluorescence was measured for each cell type overtime. The fluorescence measured in the parental line at 144 hours postplating was taken as the maximum reading (100%) and all prior readings were calculated as a percentage of this time point (normalized as a percentage of the parental line). The results are depicted in Fig. 2.

Recombinant human AMACR-maltose binding protein fusion purification

The plasmid vector (pMal-C2x, New England Biolabs) with human AMACR cloned after an *N*-terminal maltose binding protein (MBP) was a generous gift of Ferdinandusse and colleagues (9). The plasmid was transformed into chemically competent *E. coli* (TB1 strain) and recombinant protein was purified according to the manufacturer's protocol (pMal Purification Kit, New England Biolabs). After elution from the maltose column (MBPHiTrap HP maltose column, GE Healthcare Biosciences Corp.), the single eluted peak of recombinant protein was dialyzed for 1–4 hours against 1 L of 100 mmol/L Na/K/Pi buffer pH 7.25 (referred to hereafter as reaction buffer) by using slide-a-lyzer dialysis cassettes (10 kDa cutoff, ThermoFisher). The dialysis cassette was then transferred to 3 L of reaction buffer and dialyzed overnight. The following day the dialyzed lysate was quantified by the BCA protein assay kit. In addition, the recombinant AMACR-MBP protein was quantified by densitometry analysis.

High-throughput screen

[2,3-^{3}H] Pri-CoA was purchased from Moravek Biochemicals with a specific radioactivity of 4.7 Ci/mmol. For the purposes of this assay, the specific radioactivity was reduced to 60 Ci/mol by dilution with unlabeled Pri-CoA. Pristanic acid was purchased from Larodan and was ligated with CoA and purified according to published procedures (1, 2). This substrate exhibited nonspecific binding to polypropylene. To improve recoveries, 0.125 mg/mL agarose–purified bovine serum albumin (BSA; Sigma-Aldrich) was added to the reaction buffer for both experimental and control wells (referred to as complete reaction buffer). Library preparation: The Johns Hopkins Drug Library (JHDL) was diluted from the master plates [100% dimethyl sulfoxide (DMSO)] into 1X PBS at a final concentration of 500 μmol/L. The requested compounds (Diversity Set 2 and Natural Products Set) from the NCI/Developmental Therapeutics Program (DTP) Open Chemical Repository (http://dtp.cancer.gov) arrived as 10 mmol/L solutions in 100% DMSO and were diluted to 500 μmol/L in reaction buffer (without BSA, final DMSO concentration of 5%). All library plates were stored at −20°C until use, at which time they were thawed and vigorously shaken to redissolve any precipitates. The complete assay setup is described in detail in the Supplementary Material, but is summarized here and in Fig. 3. The enzymatic reaction is set up in a 96-well PCR plate with a total reaction volume of 25 μL. A total of 0.3 μmol/L AMACR-MBP is incubated with 100 μmol/L of library compound (1% DMSO) in the presence of 150 μmol/L [2, 3-^{3}H] Pri-CoA for 30 minutes at 37°C on a 96-well PCR machine. Buffer only (zero AMACR) controls are included in each plate setup as background controls. In addition, column A for each plate is used as an AMACR only (100% activity) control and column H is used as a positive AMACR inhibitor (DEPC; ref. 2) control. During the incubation, a 96-well SPE (Strata C18C Plate, Phenomenex) is conditioned with acetonitrile and equilibrated with reaction buffer on a vacuum manifold. After 30 minutes, the reaction is acid quenched, neutralized, diluted to 100 μL, and then transferred to the SPE plate. Each well of the reaction plate is then washed twice and the washes are transferred to their respective wells. The total postreaction volume is 300 μL per SPE well. Vacuum is applied and the reaction is pulled through the SPE, retaining unreacted substrate and allowing [^{3}H] H2O product to pass into the collection

Published OnlineFirst March 25, 2011; DOI: 10.1158/1535-7163.MCT-10-0902

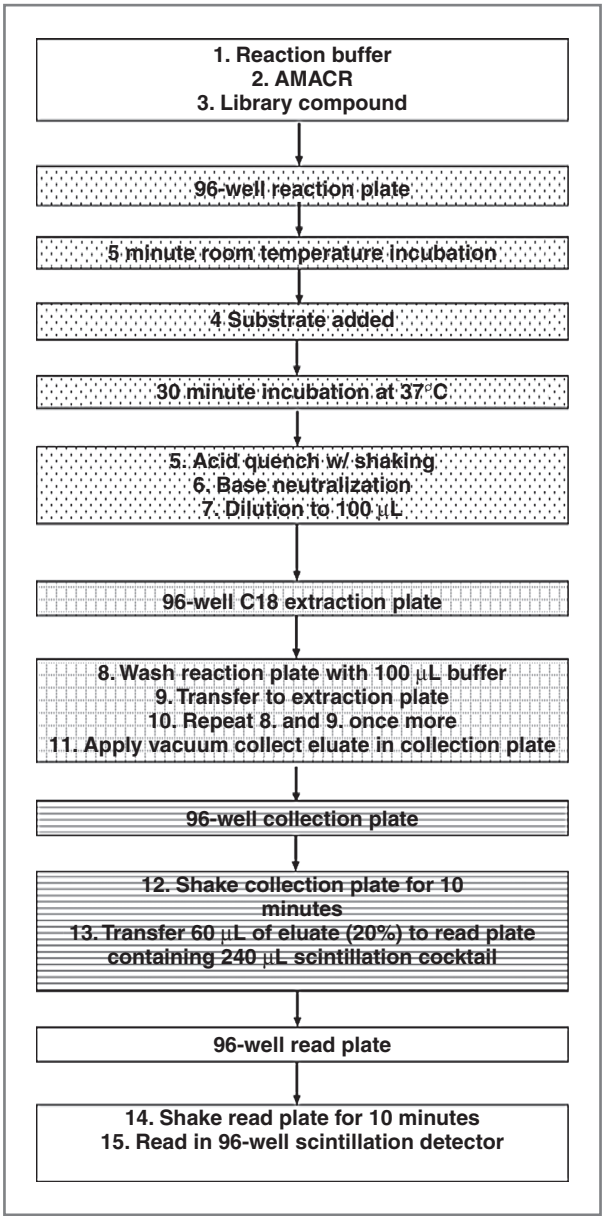

Figure 3. Schematic flowchart of novel HTS for AMACR inhibitors.

plate. A total of 60 μL of the eluate from each well is then transferred to a reading plate containing liquid scintillation fluid. The read plate is then sealed, vortexed, and read in a 96-well scintillation detector (MicroBeta Jet, Perkin-Elmer) by using a dwell time of 2 minutes per well and the same set of efficiency [counts per minute to disintegrations per minute (DPM)] standards for every plate. After the entire plate is read, the background is corrected by removing the average counts from background wells. The fractional activity (A_I/A_0) was then calculated for each library position by dividing the library DPM by the 100% activity control for that row (A column). Any well with fractional activity less than 0.8 indicates a compound that is least 20% inhibitory. Such compounds were considered worthy of further validation (Supplementary Tables S1 and S2).

HTS validation

The K_m and the V_{max} for [2, 3-^{3}H] Pri-CoA (Fig. 4) was determined by setting up 185 μL reactions at various concentrations of substrate (1, 5, 10, 15, 25, 50, 75, 100, 150, 200, 300, and 400 μmol/L) from which 20 μL aliquots were taken at time points of 0, 15, 30, 60, 120, 300, 420, 600, and 900 seconds. All of the concentrations tested had the same specific radioactivity (60 Ci/mol). The reactions were carried out by 0.3 μmol/L AMACR-MBP in microcentrifuge tubes at 37°C using complete reaction buffer (+BSA) and were initiated by the addition of enzyme to the reaction tube. After the withdrawal of each 20 μL aliquot at its designated time, the aliquot was immediately dispensed into 1 well of a 96-well plate containing 10 μL of 2 mol/L HCl to quench the reaction. Also, background controls without AMACR-MBP were set up for each time point and processed along with each experimental time point. Once the aliquots were added to the quench plate, they were processed as described for the wells in the library screen (e.g., neutralization, dilution to 100 μL, transfer to SPE plate, etc.). By using specific counts per minute to DPM standards, the number of DPM produced per unit of time was calculated and the rate of reaction determined for all concentrations tested. These concentration-dependent rates were then directly plotted and were fit to the Michaelis–Menten equation to calculate the kinetic parameters, as shown in Fig. 4 (GraphPad).

HTS candidate inhibitor validation

All library compounds that showed fractional activity of less than 0.8 were verified first by reproducing the initial high-throughput screen (HTS) screen. The initial candidate inhibitors were verified at least twice before further validation (data not shown). In the case of the JHDL,

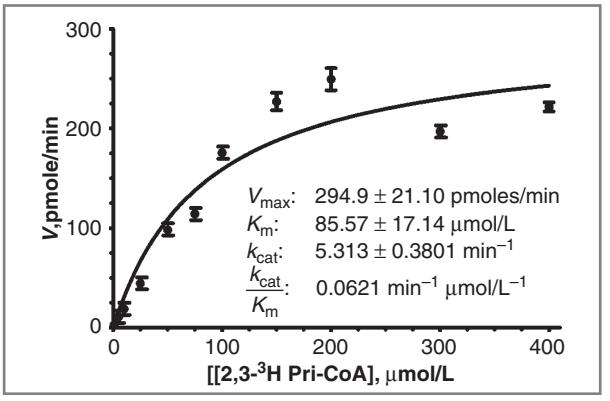

Figure 4. Kinetic analysis of AMACR-MBP purification direct plot with nonlinear regression of substrate-dependent velocity curve of AMACR-MBP incubated with [2, 3-^{3}H] Pri-CoA. Error bars indicate SEM.

Published OnlineFirst March 25, 2011; DOI: 10.1158/1535-7163.MCT-10-0902

Table 1. Novel inhibitors of AMACR discovered by HTS structures, IC_{50} values, and LD_{50} values of best inhibitors (1–8) discovered

		IC_{50} (±Std.Err)	LD_{50} (±Std. Err)
1	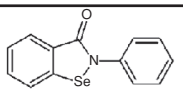 Ebselen	2.789 ± 1.341 μmol/L	LAPC4: 98.43 ± 1.038 μmol/L LNCaP: 71.96 ± 1.106 μmol/L PC3: 332.3 ± 1.015 μmol/L WPMY1: 467 ± 1.017 μmol/L
2	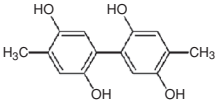 DMPMB 2-(2,5-dihydroxy-4-methylphenyl)-5-methyl benzene-1.4-diol	4.341 ± 1.402 μmol/L	LAPC4: 58.78 ± 1.058 μmol/L LNCaP: 116.9 ± 1.033 μmol/L PC3: 101.1 ± 1.034 μmol/L WPMY1: 117.6 ± 1.011μmol/L
3	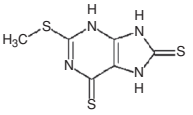 MSDTP 2-methylsulfanyl-7,9-dihydro-3H-purine-6,8-dithione	8.995 ± 1.949 μmol/L	
4	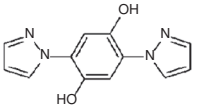 DPZBD 2,5-di(pyrazol-1-yl)benzene-1,4-diol	9.795 ± 1.700 μmol/L	
5	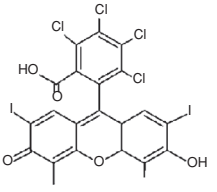 Rose Bengal	10.00 ± 1.155 μmol/L	
6	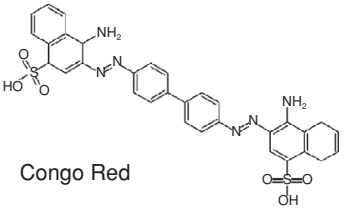 Congo Red	17.37 ± 1.256 μmol/L	
7	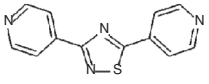 DPTD 3,5-di(pyridin-4-yl)-1,2,4-thiadiazole	84.69 ± 1.247 μmol/L	
8	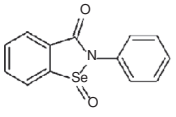 Ebselen Oxide	0.7951 ± 1.242 μmol/L	
9	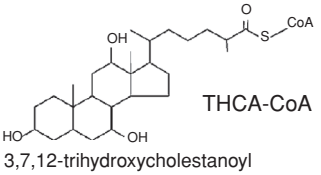 THCA-CoA 3,7,12-trihydroxycholestanoyl Coenzyme A	772.6 ± 1.991 μmol/L	

NOTE: Capitalized letters represent the acronym of the compound as used in the article. Compound 9 included for reference as a known substrate.

Published OnlineFirst March 25, 2011; DOI: 10.1158/1535-7163.MCT-10-0902

candidate inhibitors that were distinct single chemical entities and were available for purchase were obtained and their inhibitory capacities tested in a small-scale IC_{50} (inhibitory concentration) experiment by using the conditions identical to the HTS assay except that the compound concentration included 1, 10, 50, 100, 200, 500, and 1,000 μmol/L concentrations (data not shown). If a dose-dependent inhibition could be observed in that assay, then more rigorous follow-up was pursued. Based on this analysis and considerations of chemical structures, only ebselen, congo red, and rose bengal (Table 1) warranted further study. For compounds identified from the NCI/DTP Open Chemical Repository, validation was carried out in the exactly as for the JHDL. 2-(2,5-dihydroxy-4-methylphenyl)-5-methyl benzene-1, 4-diol (DMPMB), 2-methylsulfanyl-7,9-dihydro-3H-purine-6,8-dithione (MSDTP), 2,5-di(pyrazol-1-yl)benzene-1,4-diol (DPZBD), and 3,5-di(pyridin-4-yl)-1,2,4-thiadiazole (DPTD; Table 1) were chosen for rigorous follow-up and 1 to 10 mg requests were made from the NCI/DTP Open Chemical Repository (http://dtp.cancer.gov). All of the received compounds were dissolved in 100% DMSO at 25 mmol/L concentrations kept at −20°C until use. Any subsequent dilutions were also made into 100% DMSO to maintain the solubility.

AMACR inhibitor IC_{50} determination

Library compounds (Fig. 5) were tested over a broad range of concentrations (1–1,000 μmol/L, and in addition 1–750 nmol/L for ebselen/ebselen oxide) in triplicate. While the inhibitor concentration for those experiments was varied, the substrate concentration was held constant at 100 μmol/L, the AMACR-MBP at 0.3 μmol/L, and the DMSO concentration varied from 2% to 6%. Each set of reactions was set up on the same reaction plate to keep variability to a minimum. The reactions were set up by adding the necessary amount of complete reaction buffer (13.5–14.25 μL) to the wells of the reaction plate, then the inhibitor was added at the desired concentration (0.5–1.5 μL) giving a total volume of 15 μL. Next 5 μL of 500 μmol/L [2, 3-^{3}H] Pri-CoA was added to the wells, and finally, the reaction was initiated by the addition of 5 μL of 1.5 μmol/L AMACR-MBP to each well. The reactions were mixed via pipetting. All downstream processing procedures were carried out as detailed for the HTS assay. After the reading step, the fractional activity was calculated as described before and the data were analyzed by 3 parameter log(inhibitor) versus response analysis (GraphPad). The results of these analyses are shown in Table 1 (all IC_{50} curves are given in Supplementary Fig. S3).

Dialysis resistant inhibition by candidate inhibitors

A total of 400 μL preincubations were set up with 0.375 μmol/L AMACR-MBP and the concentration of each inhibitor was chosen so that inhibition would be measurable before 1 L dialysis, but would be below an IC after dialysis. The concentrations used were as follows: 25 μmol/L ebselen, 200 μmol/L DMPMB, 400 μmol/L MSDTP, 50 μmol/L DPZBD, 50 μmol/L DPTD, and 1.6% DMSO control. Preincubations were allowed to continue for 30 minutes on ice and then 200 μL was removed from each preincubation and injected into a slide-a-lyzer dialysis cassette (10 kDa cutoff, ThermoFisher). The cassettes were then separately dialyzed against 1 L of reaction buffer overnight. The remaining preincubation reaction was placed at 4°C overnight By assuming complete dialysis, the postdialysis concentration of each compound is: 5 nmol/L ebselen, 40 nmol/L DMPMB, 80 nmol/L MSDTP, 10 nmol/L DPZBD, and 10

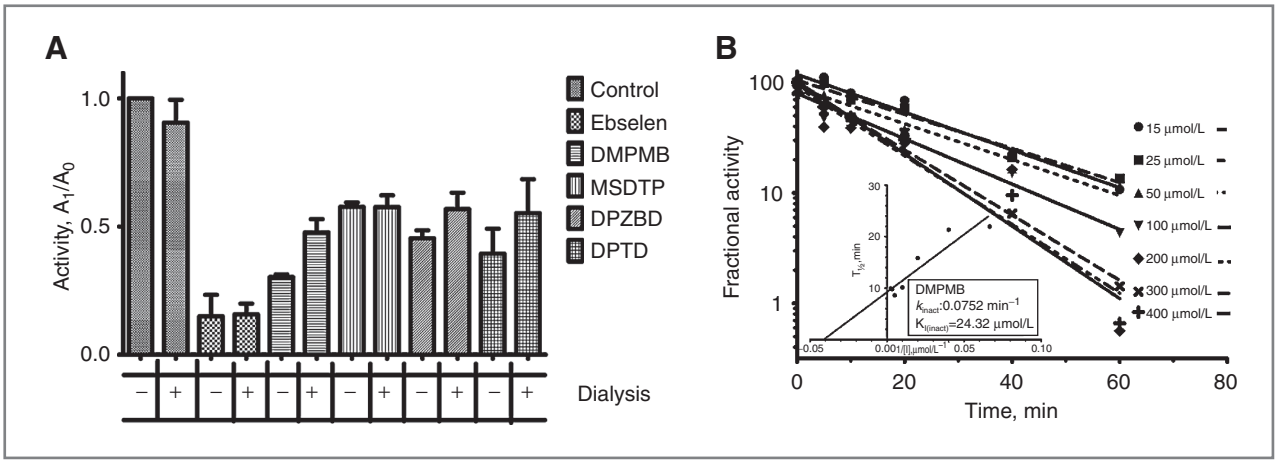

Figure 5. Time-dependent inactivation of AMACR. A, AMACR-MBP was incubated with each inhibitor at the following concentrations: 25 μmol/L ebselen, 200 μmol/L DMPMB, 400 μmol/L MSDTP, 50 μmol/L DPZBD, 50 μmol/L DPTD, or 1.6% DMSO control and then dialyzed overnight against 1 L reaction buffer. This dialysis could not recover enzymatic activity, indicating inactivation of the enzyme by the inhibitor. B, inhibition progress curves for DMPMB. DMPMB is preincubated with AMACR-MBP prior reaction initiation. Fractional activity (enzymatic activity with inhibitor/activity without) decreases with increasing preincubation time. Kitz–Wilson transformation of inhibition progress curves allows calculation of k_{inact} and $K_{I(inact)}$.

Published OnlineFirst March 25, 2011; DOI: 10.1158/1535-7163.MCT-10-0902

nmol/L DPTD. The following day the UV-visible spectra for each compound, both before and after dialysis, were scanned to determine whether there was any absorbance attributable to the inhibitor remaining in the dialyzed samples. The presence of remaining inhibitor after dialysis could not be detected for any compounds (DPZBD had no detectable absorbance peak before or after dialysis; data not shown). Next, 20 μL of both the dialyzed and undialyzed preincubations was added to 5 μL of 500 μmol/L [2, 3-^{3}H] Pri-CoA in a 96-well plate (final concentrations of AMACR-MBP 0.3 and 100 μmol/L [2, 3-^{3}H] Pri-CoA), and the reactions with AMACR-MBP were done as described before for the HTS assay. These dialysis experiments were undertaken on 3 different occasions. Dialysis against a greater volume of reaction buffer was attempted and did not change the results (data not shown). The fractional activity for both the undialyzed and dialyzed samples was calculated as described earlier. Dialysis could not recover AMACR activity after preincubation (Fig. 5A).

Kitz–Wilson analysis

In a 37°C 96-well plate, inhibition reactions were set up containing DMPMB concentrations from 0 to 400 μmol/L and 5 μmol/L AMACR-MBP. Inhibition was initiated by the addition of AMACR-MBP; immediately after which (time point zero), a 2 μL aliquot was removed and diluted into 98 μL of reaction buffer containing 150 μmol/L [2, 3-^{3}H] Pri-CoA (a 50-fold dilution reducing the final AMACR-MBP concentration to 100 nmol/L). These enzymatic reactions were allowed to proceed for 30 minutes before quenching and processing as described before for the HTS. Additional aliquots were withdrawn from the inhibition reaction at subsequent time points and diluted. Data analysis was done as described by Kitz and Wilson (27, 28). The extent of inactivation occurring on preincubation in the inhibition reaction is measured relative to time-matched control wells without inhibitor by simply dividing the background corrected DPM from the experimental (% A_I) well by their control well (% A_C; expressed as a percentage), giving a percent activity remaining. Enzymatic reaction progress curves were generated by graphing the log of the percent of activity remaining versus preincubation time before dilution (Fig. 6B). Linear regression analysis of the reaction progress curves allows for the calculation of the inactivation half-life ($T_{1/2}$, time to a 50% reduction in the experimental activity). Linear regression of the $T_{1/2}$ values versus $[I]^{-1}$ yields an equation allowing for the calculation of the inactivation rate ($k_{inact} = \ln 2/y$-intercept) and the $K_{I(inact)}$ ($-1/x$-intercept; Fig. 6B, inset). Identical experiments were carried out for ebselen (Supplementary Fig. S4).

In vitro LD_{50} measurements for DMPMB and ebselen

PC3 and LNCaP cell lines were purchased from ATCC, WPMY1 cells were acquired from the laboratory of Dr. S.R. Denmeade (29). LAPC4 cells are described before. Western blotting for AMACR expression and loading controls for these cell lines were done identically as for LAPC4 before and the results are depicted in the inset of Fig. 6A (complete blots are in Supplementary Fig. S5).

To determine the concentration of ebselen or DMPMB that is lethal to 50% of cells (LD_{50}), 10,000 cells of each type were plated in triplicate in zero fluorescence tissue culture treated 96-well plates (BD Biosciences). The cells established overnight and the following day their media were replaced with media containing either ebselen or DMPMB in a concentration range of 0 to 500 μmol/L or 0 to 400 μmol/L, respectively. After 48 hours, the alamarBlue assay for viability was done as described for

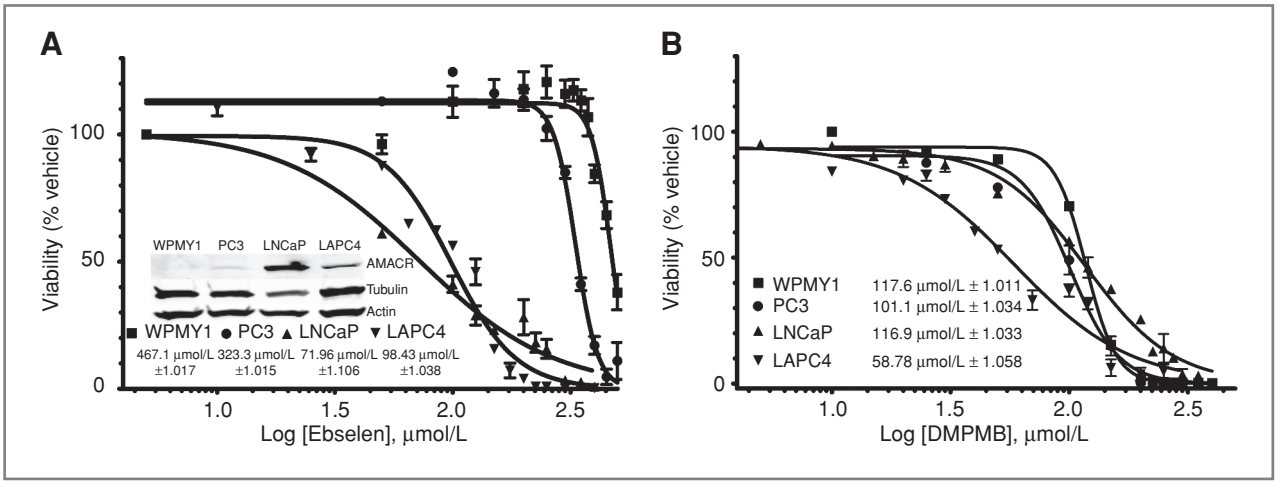

Figure 6. *In vitro* cytotoxicity studies of ebselen and DMPMB. A, LD_{50} curves for ebselen in 3 prostate cancer cell lines (PC3, LNCaP, and LAPC4) and 1 normal prostate fibroblast cell line (WPMY1). All data points are normalized as a percentage of their respective vehicle controls. Inset, Western blot analysis of AMACR expression in 4 cell lines, showing increasing ebselen sensitivity with increasing AMACR expression (tubulin and actin blotted as loading controls). B, LD_{50} curves for DMPMB as in A.

Published OnlineFirst March 25, 2011; DOI: 10.1158/1535-7163.MCT-10-0902

LAPC4 earlier. The viability was calculated as a percent of the no inhibitor control for each cell type, after correcting for media only background fluorescence. The percent viability as a function of increasing log of inhibitor concentration was then analyzed by a least-squares fit for nonlinear regression with a variable slope (4 parameter) and constraining the bottom to zero (GraphPad). The results of these analyses can be seen in Fig. 6A and B.

Results

Stable shRNA-mediated AMACR knockdown validates AMACR as a therapeutic target

Previously, we have studied the effect of substrate-based AMACR inhibitors on different prostate cancer cell lines with variable levels of AMACR expression (26). In addition, we have transiently attenuated AMACR expression through the use of short interfering RNA (14). To extend these analyses, here, we report the use of commercial lentiviral particles to stably reduce the expression of AMACR.

LAPC4 cells were transduced with lentivirus containing an shRNA construct targeting AMACR (LAPC4 AMACRKO). As a parallel control, cells were also transduced with lentivirus containing an shRNA construct targeting no known gene in the human genome (vector). To assess the ability of the shRNA to reduce AMACR expression, a Western blot was prepared by lysates from the parental, vector, and AMACRKO cell lines (Fig. 2, inset). As seen in Fig. 2, the shRNA construct rendered AMACR protein expression undetectable by immunoblotting. To test the growth effect of biochemical AMACR depletion, parental, vector, and AMACRKO cells were plated at equal density in 96-well plates and their growth was measured for 6 days by the alamarBlue assay. There is a statistically significant difference between the vector and AMACRKO cell lines ($P < 0.05$, 2-tailed t test), whereas no significant difference exists between vector and LAPC4 parental cell lines (Fig. 2). Identical studies were carried out by the prostate cancer cell line LNCaP (Supplementary Fig. S1). Our observations confirm that reducing AMACR expression slows prostate cancer cell growth, providing further impetus to develop small molecules that can inhibit AMACR activity.

Purification of enzymatically active AMACR from *E. coli*

A recombinant expression vector containing the human AMACR cDNA with an *N*-terminal MBP tag was obtained (AMACR-MBP; ref. 9). By using that vector, milligram quantities of AMACR-MBP were routinely purified. To guard against the possibility that nonspecific carryover from the *E. coli* host strain may be providing enzymatic activity similar to that of AMACR, site-directed mutagenesis was used to create a known inactivating mutation within the AMACR construct, changing serine 52 to proline (9). That mutation eliminated all measurable AMACR activity from our preparations, indicating that all measured AMACR activity was from AMACR-MBP and not from a contaminant (data not shown).

To ensure that we were purifying enzymatically active AMACR-MBP, an HPLC-based assay was used (6). It has been shown that diastereomers of the AMACR substrate (25 *R,S)* 3,7,12-trihydroxycholestanoyl CoA (THCA-CoA) can be separated and collected independently of each other via reverse phase C18 HPLC. The separated diastereomers (either 25*R* or 25*S*) can then be incubated in the presence of AMACR and the conversion of 1 enantiomer to the other can be monitored over time via HPLC. Using that assay AMACR-MBP was confirmed as enzymatically active (or inactive in the case of the S52P mutant; Supplementary Fig. S2). Although this assay is adequate for validation and comparison of enzymatic preparations, the retention times for the separation of diastereomers and the amount of processing involved make this assay impractical for use in an HTS.

Development of an HTS for AMACR inhibitors

None of the current assays for AMACR activity have been adapted to a multiwell screening format (1–6, 9, 15, 25, 26). We established a 96-well plate assay for AMACR activity on the basis of a previously published assay for measuring cytochrome p450 activity (30, 31). In the plate-based assay, the enzyme (0.3 μmol/L) is incubated with 150 μmol/L labeled substrate [2, 3-^{3}H] Pri-CoA (Fig. 1) in the presence or absence of 100 μmol/L of a library compound producing ^3H_2O as a measure of enzymatic activity (Fig. 3). The reaction mixture is transferred to a C18 SPE plate that allows the liberated tritiated water to be separated from any unmetabolized substrate. The level of enzymatic activity can be measured through the use of 96-well microplate scintillation counting. AMACR inhibition is quantified by comparing the number of DPM from enzymatic product to plate controls containing no inhibitor or 100 μmol/L of a known inhibitor (DEPC; ref. 2).

Kinetic parameters of the HTS

The kinetic parameters for labeled substrate in the assay were determined (Fig. 4). Initial reaction rates were determined by incubating 0.3 μmol/L AMACR-MBP with varying concentrations of [2, 3-^{3}H] Pri-CoA (specific radioactivity was maintained at 60 Ci/mole) from which aliquots were taken at time points from 0 to 900 seconds. Those samples were then treated as individual wells in our assay and processed as described earlier. The concentration-dependent time points were used to calculate reaction rates. These rates were then directly plotted against concentrations and kinetic parameters calculated by nonlinear regression (Fig. 4). The calculated kinetic values [V_{max}: 294.9 ± 21.10 pmoles/minute (SEM); K_m: 85.57 ± 17.14 μmol/L (SEM)] are similar to other published reports using human AMACR (1, 3).

Published OnlineFirst March 25, 2011; DOI: 10.1158/1535-7163.MCT-10-0902

HTS of 4,896 unique small molecules

JHDL contains 3,280 distinct molecules the majority of which are drugs currently approved by the U.S. Food and Drug Administration, or its foreign counterparts, in addition to numerous other bioactive compounds (32). Those compounds were screened at a final concentration of 100 μmol/L. Any compound that diminished the fractional activity by 20% or more was considered as a candidate inhibitor (Supplementary Table S1). Of the 3,280 compounds screened in this library, 167 met the criteria of a minimum of 20% inhibition (5.1% positive hit rate), and of these, 3 were chosen for further analysis (Rose Bengal, Congo Red, and Ebselen; Table 1). In screening the JHDL, the detection of mercury and copper containing compounds was an internal validation of the reliability of the assay (along with *N*-ethylmaleimide), as these compounds have been reported to be inhibitory elsewhere (Supplementary Table 1; ref. 2). AMACR has been shown to have an active site histidine (His122; ref. 8). Therefore, the discovery of Rose Bengal, a compound known to selectively inhibit enzymes with active site histidine residues, indicated that the discovered compounds were relevant to AMACR biochemistry (33).

After screening the JHDL, 2 other small libraries of compounds from the NCI/DTP Open Chemical Repository (http://dtp.cancer.gov/) were obtained. The natural products set is composed of 235 structurally diverse compounds. The diversity set 2 library contains 1,324 compounds that were chosen by the NCI/DTP on the basis of several criteria as potential pharmacophores for biological activity. The screen of both of those libraries was done identically to that of the JHDL, and the candidate inhibitors meeting the 20% inhibitory cutoff are listed in Supplementary Table S2. Of the 1,559 compounds from the NCI/DTP Open Chemical Repository, 37 met the cutoff of a minimum of 20% inhibition (2.4% positive hit rate) and upon subsequent validation, only 4 were chosen for further follow-up (Table 1). The detection of the inhibition of AMACR-MBP by mitoxantrone in both the JHDL and the NCI/DTP libraries indicates good reproducibility across library platforms (Supplementary Tables S1 and S2).

Candidate inhibitor validation

After reproducing the results from the initial screen, several of the most potent inhibitors were subjected to subsequent analysis (Table 1). The potency of the candidate inhibitors was validated by determining their IC_{50} values. The IC_{50} values for characterized candidate inhibitors are listed in Table 1 and the IC_{50} curves themselves are in Supplementary Fig. S3. Trihydroxycholestanoyl CoA (compound 9) is a well-characterized substrate and was included as a positive control for inhibition and as external validation of the SPE-based assay (1, 2, 6). Ebselen oxide was tested as a commercially available derivative of the most potent inhibitor, ebselen, and showed an equivalent ability to inhibit AMACR (Table 1). As the first reported inhibitors of AMACR that are not substrates containing SCoA, the IC_{50} values for these compounds (1–8) ranged from 0.80 to 84.69 μmol/L, which compares favorably to recently reported competitive inhibitors of the enzyme (K_i: 0.9–137 μmol/L), all of which are based on known AMACR substrates and contain the cell impermeable CoA moiety (10).

Time-dependent nondialyzable inhibition by candidate inhibitors

During the validation experiments for ebselen, it was observed that the degree of inhibition increased, depending on whether the reaction was initiated with substrate or enzyme. The only difference between those 2 conditions is the amount of time that the enzyme is preincubated with inhibitor before the addition of substrate (reaction initiation). Enzyme initiated reactions had no preincubation period and substrate initiated reactions had preincubation times of 5 minutes or more. In the presence of ebselen, a preincubation time of 5 minutes or more reduces the fractional activity of AMACR-MBP from approximately 50% to just above background, showing a time-dependent component to ebselen inhibition (Supplementary Fig. S3, inset).

Published reports showing that ebselen is capable of covalent modification of proteins suggest that ebselen may cause an irreversible inhibition of AMACR that is resistant to dialysis (34, 35). To assess this possibility, experiments were set up whereby the AMACR-MBP was preincubated with inhibitor for 30 minutes at 4°C, dialyzed overnight, and then exposed to the substrate. The amount of activity remaining after dialysis was then compared with controls to determine to what extent the dialysis could recover AMACR-MBP activity. As shown in Fig. 6A, for none of the inhibitors tested, could activity be recovered. The only inhibitor for which there seemed to be any statistically significant recovery of activity was DPZBD, and even this was only marginal (Fig. 6A). To ensure that the compounds themselves were capable of being dialyzed, the UV-visible spectrum of each reaction was checked before and after dialysis and in all cases, the absorbance peaks of the inhibitors seen before dialysis were not seen after dialysis (data not shown). Neither congo red nor rose bengal could be included in that analysis as both have been shown to form nondialyzable aggregates (36, 37).

The dialysis data (Fig. 5A) suggest that the AMACR inhibitors may be acting as covalent inactivators. To further investigate this possibility, we chose to carry out Kitz–Wilson analyses for our top 2 inhibitors (compounds 1–2, Table 1; refs. 27, 28). Inhibition progress curves for compound 2 (DMPMB) were linear with increasing time and concentration (Fig. 5B, inset), and upon Kitz–Wilson transformation yielded an inactivation rate ($k_{i(\text{inact})}$) of 0.07521(±0.01067) per minute and a $K_{I(\text{inact})}$ of 24.32(±3.07) μmol/L (Fig. 5B). Unfortunately, the inhibition progress curves for ebselen are curvilinear

Published OnlineFirst March 25, 2011; DOI: 10.1158/1535-7163.MCT-10-0902

and do not fit the standard Kitz–Wilson model; and transformation of the linear portion of these curves results in a negative $k_{i(inact)}$ (Supplementary Fig. S5). It has been suggested in the literature that inhibitors with this pattern of Kitz–Wilson analysis may be indicative of multiple binding events (either multiple inactivator binding sites or multiple inactivator molecules binding to a single site; ref. 38).

Noncysteine-dependent inactivation by ebselen

Ebselen has been shown to covalently modify cysteine residues in several proteins (34, 35). However, it has not been shown that any cysteine residues play a role in AMACR catalysis (7, 8). To gain further insight into the mechanism of inhibition by ebselen, we sought determine whether or not ebselen-mediated inhibition (100 μmol/L) could be prevented by preincubation of AMACR with cysteine-specific alkylating agents [5 mmol/L tributylphosphine (TBP), 15 mmol/L iodoacetamide (IAA), TBP + IAA, 20 mmol/L dithithreitol (DTT)]. The enzyme was either first exposed to the alkylating agents and then directly incubated with ebselen before enzymatic measurement; or the AMACR was dialyzed after exposure to alkylators (removing excess alkylator) and then ebselen was added. Both the enzymatic activity and the sensitivity to inhibition with alkylator/ebselen were tested (Supplementary Fig. S6). The data for TBP indicate that TBP coincubated with ebselen can protect AMACR from inhibition, presumably by alkylation of ebselen by excess TBP rather than direct protection of AMACR. When the excess TBP is dialyzed away, the enzyme is still sensitive to inhibition by ebselen. While IAA itself did slightly inhibit AMACR activity (approximately 83% activity remaining after dialysis), it could not protect AMACR from ebselen-mediated inhibition. The combination of TBP and IAA was slightly inhibitory after dialysis (approximately 81% activity, similar to IAA alone) and did offer some degree of protection from ebselen before dialysis (approximately 50% activity remaining, most likely attributable to the reaction of TBP with ebselen), but this protection was not present after dialysis. DTT did not protect AMACR from inhibition during coincubation of both ebselen and DTT. The fact that none of the cysteine-specific reactive compounds affected AMACR activity confirms that there is not likely a cysteine-mediated contribution to catalysis. Their failure to protect AMACR from ebselen inhibition indicates that cysteine modification by ebselen may not be the cause of AMACR inhibition

In vitro toxicity for ebselen and DMPMB

AMACR inhibitors may have differential effects on cells on the basis of the amount of AMACR protein being expressed. As a baseline for comparison, 4 immortalized human prostate cell lines with differing levels of AMACR expression were tested for toxicity in the presence of ebselen and DMPMB (Fig. 6A and B). WPMY1 is a nontumorgenic human prostate stromal myofibroblast cell line that has undetectable AMACR protein by Western blot analysis (Fig. 6A, inset; ref. 29). PC3, LAPC4, and LNCaP are 3 commonly used prostate cancer cell lines listed in order of increasing AMACR expression (Fig. 6A, inset). For all 4 cell lines, LD_{50} experiments were carried out by plating each line in triplicate at equal density in 96-well plates. The cells were then allowed to establish overnight before exposure to increasing quantities of either ebselen or DMPMB. For ebselen, the measured LD_{50} decreases with increasing AMACR expression (LD_{50}s, WPMY1: 467.1 ± 1.017 μmol/L, PC3: 332.3 ± 1.015 μmol/L, LAPC4: 98.43 ± 1.038 μmol/L, LNCaP: 71.96 ± 1.106 μmol/L, Fig. 7A). This trend did not seem when measuring the LD_{50} for DMPMB in these cell lines: WPMY1: 117.6 ± 1.011 μmol/L, PC3: 101.1 ± 1.034 μmol/L, LAPC4: 58.78 ± 1.058 μmol/L, 116.9 ± 1.033 μmol/L (Fig. 6B).

Discussion

Recent controversy about prostate cancer screening has highlighted the need for noninvasive intraprostatic detection and monitoring of cancer (23, 24, 39). A tissue biomarker of prostate cancer like AMACR provides an ideal candidate for targeted molecular imaging and chemotherapy (19, 21). AMACR has been shown to be overexpressed in prostate adenocarcinoma by at least 10-fold over normal tissue and is used as an immunohistochemical marker of prostate cancer (11). To further exploit AMACR overexpression for both therapeutic and imaging purposes, we have created the first published 96-well–based assay to screen for inhibitors and report the first inhibitors for AMACR that are not SCoA-containing substrate analogs (Figs. 3 and Table 1).

Unlike its predecessors, our assay is not a single-condition assay and can therefore be used to screen large numbers of compounds, concentrations, and conditions at the same time. Until now a high-throughput assay for AMACR activity has remained elusive for a variety of reasons, the most obvious being the fact that AMACR is a racemase that requires an SCoA moiety in its substrates (Fig. 1). As a racemase, AMACR is responsible for the stereoinversion of a single chiral center, and as such does not produce a product that is easily distinguishable from its substrate. There have been only 2 other published multiwell screens for inhibitors of any known racemase (40, 41). We show here a 96-well plate–based AMACR assay capable of screening thousands of compounds and finding unique chemical entities that do not face the limitations of substrate-based competitive inhibitors (26).

While validating the most potent inhibitors (ebselen and DMPMB, Table 1), we observed that this inhibition is both time dependent and irreversible by dialysis (Fig. 5, Supplementary Figs. S3 and S4). Furthermore, we show that both DMPMB and ebselen are irreversible inactivators of AMACR, the first uncompetitive AMACR inhibitors reported.

Ebselen has been previously reported to covalently modify several other proteins, act as a peroxidase, have

Published OnlineFirst March 25, 2011; DOI: 10.1158/1535-7163.MCT-10-0902

anti-inflammatory properties, and be neuroprotective (34, 35, 42–44). It is important to consider that all of the aforementioned characteristics are not only beneficial but considered chemopreventative for cancer (45). In addition, ebselen has been used in 2 different clinical trials as a neuroprotective agent (44, 46). Neuroprotective doses of ebselen (300 mg/day) were well tolerated and could reach therapeutic levels through oral dosing (44, 46). Those pharmacologic properties make ebselen amenable to use in the setting of prostate cancer. To this end, we have determined the LD_{50} for ebselen and DMPMB in a variety of prostate cell lines and have observed some interesting trends. For ebselen, cells that express more AMACR seem to be more sensitive to ebselen-mediated cell death (Fig. 6). There is a 5-fold difference in LD_{50} between the highest AMACR expressing cell line (LNCaP) and the lowest AMACR expressor (WPMY1). In addition, we show in Supplementary Fig. S7 that both ebselen and DMPMB induced necrotic cell death. One possible explanation for this observation is that cell lines with high AMACR expression may become dependent on AMACR activity (for example, branch chain lipid oxidation may provide additional reducing equivalents or intermediary metabolites like acetyl-CoA) and are then sensitized to ebselen-mediated AMACR inhibition. The observation that the AMACR inhibitors ebselen and DMPMB cause necrotic cell death (Supplementary Fig. S7) is consistent with another published report of metabolic inhibitors causing necrosis rather than apoptosis, and supports the possibility that AMACR overexpression may make cells dependent on metabolites derived from AMACR reliant pathways (47). This AMACR addiction is consistent with the observation that LAPC4 cells with decreased AMACR expression grow much more slowly than do the vector controls (Fig. 2). The difference in sensitivity to ebselen between cells expressing AMACR and those that do not suggests that there is a therapeutic window for specifically targeting AMACR expressing cells (cancer) while sparing the non-AMACR expressing normal tissue.

Ebselen is known to inhibit other enzymes through covalent modification of cysteine residues (34, 35). We show that preincubation of AMACR with cysteine-specific reagents (20 mmol/L DTT, 5 mmol/L TBP, or 15 mmol/L IAA) does not abrogate AMACR-MBP activity, nor does it prevent ebselen-mediated inhibition (Supplementary Fig. S6). This observation suggests that ebselen is not simply alkylating an exposed cysteine, but we hypothesize rather that it may alkylate the active site histidine (His122) specifically. Rose bengal has been reported to inhibit enzymes with an active site histidine reside, so it is perhaps not surprising that our assay discovered it to inhibit AMACR (33).

Along with its role in prostate cancer, the AMACR homolog in *Mycobacterium tuberculosis* has been intimately tied to the field of AMACR research through use of both crystal structures and the enzyme itself as a stand-in for AMACR (7, 8). It has not been established whether the homolog is required for survival, but it will be interesting to see whether our assay can be used to screen for homolog-directed antibiotics and whether any of the compounds that we have outlined here may show antibiotic activity.

Intraprostatic tumor imaging remains elusive as the conventional agent, [^{18}F] fluorodeoxyglucose with positron emission tomography, has not proved useful in prostate cancer and all other agents remain at the experimental stage (20). As covalent inactivators of AMACR, ebselen, DMPMB, and MSDTP (unpublished observation) may accumulate in areas where AMACR is highly expressed (like prostate cancer) compared with areas with little to no AMACR expression (normal tissue), suggesting that postive emission/computed tomography imagible analogs of ebselen could represent an advance over noncovalent inhibitors. Although we have only studied the properties of a single ebselen analog (ebselen oxide), there are numerous other synthetically available analogs (42, 48). We believe that our discovery of these potent inhibitors of AMACR activity warrant further preclinical investigation as imaging and chemotherapeutic agents for prostate cancer. Furthermore, the high-throughput assay that we have developed lends itself to the rapid screening of both new libraries and derivatives of the inhibitors described here.

Disclosure of Potential Conflicts of Interest

No potential conflicts of interest were disclosed.

Acknowledgments

We thank M. Rosen and Dr. S.R. Denmeade for training and use of HPLC equipment and reagents, and K.H. Burgwin for cytotoxicity discussions.

Grant Support

This work is supported by funding from the U.S. Department of Defense (W81XWH-08–1-0073, B.A.P. Wilson), the Patrick C. Walsh Prostate Cancer Research Foundation (W.B. Isaacs, B.A.P. Wilson), and the NIH (CA131702, CA92871, H. Wang, R.C. Mease, M.G. Pomper). The maintenance of JHDL (B.A. Nacev, J.O. Liu) is supported by NCI (CA122814), FAMRI, CTSA, and the Patrick C. Walsh Prostate Cancer Research Foundation.

The costs of publication of this article were defrayed in part by the payment of page charges. This article must therefore be hereby marked *advertisement* in accordance with 18 U.S.C. Section 1734 solely to indicate this fact.

Received September 30, 2010; revised December 17, 2010; accepted March 16, 2011; published OnlineFirst March 25, 2011.

References

1. Schmitz W, Albers C, Fingerhut R, Conzelmann E. Purification and characterization of an α-methylacyl-CoA racemase from human liver. Eur J Biochem 1995;231:815–22.

2. Schmitz W, Fingerhut R, Conzelmann E. Purification and properties of an alpha-methylacyl-CoA racemase from rat liver. Eur J Biochem 1994;222:313–23.

Published OnlineFirst March 25, 2011; DOI: 10.1158/1535-7163.MCT-10-0902

3. Darley DJ, Butler DS, Prideaux SJ, Thornton TW, Wilson AD, Woodman TJ, et al. Synthesis and use of isotope-labelled substrates for a mechanistic study on human α-methylacyl-CoA racemase 1A (AMACR; P504S). Org Biomol Chem 2009;7:543–52.
4. Ouazia D, Bearne SL. A continuous assay for α-methylacyl-coenzyme A racemase using circular dichroism. Anal Biochem 2010;398:45–51.
5. Sattar FA, Darley DJ, Politano F, Woodman TJ, Threadgill MD, Lloyd MD. Unexpected stereoselective exchange of straight-chain fatty acyl-CoA α-protons by human α-methylacyl-CoA racemase 1A (P504S). Chem Commun 2010;46:3348–50.
6. Cuebas DA, Phillips C, Schmitz W, Conzelmann E, Novikov DK. The role of alpha-methylacyl-CoA racemase in bile acid synthesis. Biochem J 2002;363(Pt 3):801–7.
7. Salvolainen K, Bhaumik P, Schmitz W, Kotti TJ, Conzelmann E, Wierenga RK, et al. α -Methylacyl-CoA racemase from Mycobacterium tuberculosis: mutational and structural characterization of the active site and the fold. J Biol Chem 2004;280:12611–20.
8. Bhaumik P, Schmitz W, Hassinen A, Hiltunen JK, Conzelmann E, Wierenga RK. The catalysis of the 1, 1-proton transfer by [alpha]-methyl-acyl-CoA racemase is coupled to a movement of the fatty acyl moiety over a hydrophobic, methionine-rich surface. J Mol Biol 2007;367:1145–61.
9. Ferdinandusse S, Denis S, Clayton PT, Graham A, Rees JE, Allen JT, et al. Mutations in the gene encoding peroxisomal α-methylacyl-CoA racemase cause adult-onset sensory motor neuropathy. Nat Genet 2000;24:188–91.
10. Xu J, Stolk JA, Zhang X, Silva SJ, Houghton RL, Matsumura M , et al. Identification of differentially expressed genes in human prostate cancer using subtraction and microarray. Cancer Res 2000;60:1677–82.
11. Luo J, Zha S, Gage WR, Dunn TA, Hicks JL, Bennett CJ, et al. α-Methylacyl-CoA racemase: a new molecular marker for prostate cancer. Cancer Res 2002;62:2220–6.
12. Goldstein AS, Huang J, Guo C, Garraway IP, Witte ON. Identification of a cell of origin for human prostate cancer. Science 2010;329:568–71.
13. Rubin MA, Zhou M, Dhanasekaran SM, Varambally S, Barrette TR, Sanda MG, et al. α-methylacyl coenzyme A racemase as a tissue biomarker for prostate cancer. JAMA 2002;287:1662–70.
14. Zha S, Ferdinandusse S, Denis S, Wanders RJ, Ewing CM, Luo J, et al. α-methylacyl-CoA racemase as an androgen-independent growth modifier in prostate cancer. Cancer Res 2003;63:7365–76.
15. Kumar-Sinha C, Shah RB, Laxman B, Tomlins SA, Harwood J, Schmitz W, et al. Elevated α-methylacyl-CoA racemase enzymatic activity in prostate cancer. Am J Pathol 2004;164:787–93.
16. Takahara K, Azuma H, Sakamoto T, Kiyama S, Inamoto T, Ibuki N , et al. Conversion of prostate cancer from hormone independency to dependency due to AMACR inhibition: involvement of increased AR expression and decreased IGF1 expression. Anticancer Res 2009;29:2497–505.
17. Savolainen K, Kotti TJ, Schmitz W, Savolainen TI, Sormunen RT, Ilves M, et al. A mouse model for α-methylacyl-CoA racemase deficiency: adjustment of bile acid synthesis and intolerance to dietary methyl-branched lipids. Hum Mol Genet 2004;13:955–65.
18. Zhou M, Chinnaiyan AM, Kleer CG, Lucas PC, Rubin MA. Alpha-methylacyl-CoA racemase: a novel tumor marker over-expressed in several human cancers and their precursor lesions. Am J Surg Pathol 2002;26:926–31.
19. Zlatopolskiy B, Morgenroth A, Urusova E, Kunkel FH, Dinger C, Kull T, et al. IVC-11: a tracer for targeting of α-methylacyl-CoA racemase (AMACR). J Nucl Med 2009;50:1913
20. Zaheer A, Cho SY, Pomper MG. New agents and techniques for imaging prostate cancer. J Nucl Med 2009;50:1387–90.
21. Turkbey B, Albert PS, Kurdziel K, Choyke PL. Imaging localized prostate cancer: current approaches and new developments. Am J Roentgenol 2009;192:1471–80.
22. Edwards BK, Ward E, Kohler BA, Eheman C, Zauber AG, Anderson RN, et al. Annual report to the nation on the status of cancer, 1975–2006, featuring colorectal cancer trends and impact of interventions (risk factors, screening, and treatment) to reduce future rates. Cancer 2010;116:544–73.
23. Welch HG, Albertsen PC. Prostate cancer diagnosis and treatment after the introduction of prostate-specific antigen screening: 1986–2005. J Natl Cancer Inst 2009;101:1325–9.
24. Brawley OW. Prostate cancer sreening; is this a teachable moment?J Natl Cancer Inst 2009;101:1295–7.
25. Van Veldhoven P, Croes K, Casteels M, Mannaerts G. 2-methylacyl racemase: a coupled assay based on the use of pristanoyl-CoA oxidase/peroxidase and reinvestigation of its subcellular distribution in rat and human liver. Biochim Biophys Acta 1997;1347:62–8.
26. Carnell AJ, Hale I, Denis S, Wanders RJ, Isaacs WB, Wilson BA, et al. Design, synthesis, and in vitro testing of α-methylacyl-CoA racemase inhibitors. J Med Chem 2007;50:2700–7.
27. Silverman RB. Mechanism-based enzyme inactivators. Enzyme kinetics and mechanism part D: developments in enzyme dynamics. San Diego: Academic Press; 1995p. 240–83.
28. Kitz R, Wilson IB. Esters of methanesulfonic acid as irreversible inhibitors of acetylcholinesterase. J Biol Chem 1962;237:3245–50.
29. Webber MM, Trakul N, Thraves PS, Bello-DeOcampo D, Chu WW, Storto PD, et al. A human prostatic stromal myofibroblast cell line WPMY-1: a model for stromal–epithelial interactions in prostatic neoplasia. Carcinogenesis 1999;20:1185–92.
30. Marco AD, Marcucci I, Verdirame M, Pérez J, Sanchez M, Peláez F, et al. Development and validation of a high-throughput radiometric CYP3A4/5 inhibition assay using tritiated testosterone. Drug Metabol Dispos 2005;33:349–58.
31. Di Marco A, Cellucci A, Chaudhary A, Fonsi M, Laufer R. High-throughput radiometric CYP2C19 inhibition assay using tritiated (S)-mephenytoin. Drug Metabol Dispos 2007;35:1737–43.
32. Chong CR, Chen X, Shi L, Liu JO, Sullivan DJ. A clinical drug library screen identifies astemizole as an antimalarial agent. Nat Chem Biol 2006;2:415–6.
33. Grillo FG, Aronson PS. Inactivation of the renal microvillus membrane Na+-H+ exchanger by histidine-specific reagents. J Biol Chem 1986;261:1120–5.
34. Walther M, Holzhutter HG, Kuban RJ, Wiesner R, Rathmann J, Kuhn H. The inhibition of mammalian 15-lipoxygenases by the anti-inflammatory drug ebselen: dual-type mechanism involving covalent linkage and alteration of the iron ligand sphere. Mol Pharmacol 1999;56:196–203.
35. Sakurai T, Kanayama M, Shibata T, Itoh K, Kobayashi A, Yamamoto M, Uchida K. Ebselen, a seleno-organic antioxidant, as an electrophile. Chem Res Toxicol 2006;19:1196–1204.
36. Weiser HB, Radcliffe RS. The physical chemistry of color lake formation. IV. Red Congo Acids and Red Congo Lakes. J Phys Chem 1928;32:1875–85.
37. Valdes-Aguilera O, Neckers DC. Aggregation of rose bengal ethyl ester induced by alkali metal cations in aqueous solution. J Photochem Photobiol A: Chem 1989;47:213–22.
38. Kuo DJ, Jordan F. Active site directed irreversible inactivation of brewers' yeast pyruvate decarboxylase by the conjugated substrate analog (E)-4-(4-chlorophenyl)-2-oxo-3-butenoic acid: development of a suicide substrate. Biochemistry 1983;22:3735–40.
39. Schroder FH, Hugosson J, Roobol MJ, Tammela TL, Ciatto S, Nelen V, et al. Screening and prostate-cancer mortality in a randomized European study. The N Engl J Med 2009;360:1320–8.
40. Henderickx HJW, Duchateau ALL, Raemakers-Franken PC. Chiral liquid chromatography-mass spectrometry for high-throughput screening of enzymatic racemase activity. J Chromatogr A 2003;1020:69–74.
41. Dixon SM, Li P, Liu R, Wolosker H, Lam KS, Kurth MJ, et al. Slow-binding human serine racemase inhibitors from high-throughput screening of combinatorial libraries. J Med Chem 2006;49:2388–97.
42. Bhabak K, Mugesh G. Synthesis, characterization, and antioxidant activity of some ebselen analogues. Chem Eur J 2007;13:4594–601.
43. Zhao R, Masayasu H, Holmgren A. Ebselen: a substrate for human thioredoxin reductase strongly stimulating its hydroperoxide reduc-

Published OnlineFirst March 25, 2011; DOI: 10.1158/1535-7163.MCT-10-0902

tase activity and a superfast thioredoxin oxidant. Proc Natl Acad Sci 2002;99:8579–84.

44. Saito I, Asano T, Sano K, Takakura K, Abe H, Yoshimoto T, et al. Neuroprotective effect of an antioxidant, ebselen, in patients with delayed neurological deficits after aneurysmal subarachnoid hemorrhage. Neurosurgery 1998;42:269–77.
45. Bardia A, Platz EA, Yegnasubramanian S, De Marzo AM, Nelson WG. Anti-inflammatory drugs, antioxidants, and prostate cancer prevention. Curr Opin Pharmacol 2009;9:419–26.
46. Yamaguchi T, Sano K, Takakura K, Saito I, Shinohara Y, Asano T, Yasuhara H. Ebselen in acute ischemic stroke: a placebo-controlled, double-blind clinical trial. Stroke 1998;29:12–7.
47. Zhang D, Shao J, Lin J, Zhang N, Lu BJ, Lin SC, et al. RIP3, an energy metabolism regulator that switches death from apoptosis to necrosis. Science 2009;325:332–6.
48. Parnham M, Biedermann J, Bittner C, Dereu N, Leyck S, Wetzig H. Structure-activity relationships of a series of anti-inflammatory benzisoselenazolones (BISAs). Agents Actions 1989;27:306–8.

AACR American Association for Cancer Research

Molecular Cancer Therapeutics

High-Throughput Screen Identifies Novel Inhibitors of Cancer Biomarker α-Methylacyl Coenzyme A Racemase (AMACR/P504S)

Brice A.P. Wilson, Haofan Wang, Benjamin A. Nacev, et al.

Mol Cancer Ther 2011;10:825-838. Published OnlineFirst March 25, 2011.